



SONA COLLEGE OF TECHNOLOGY

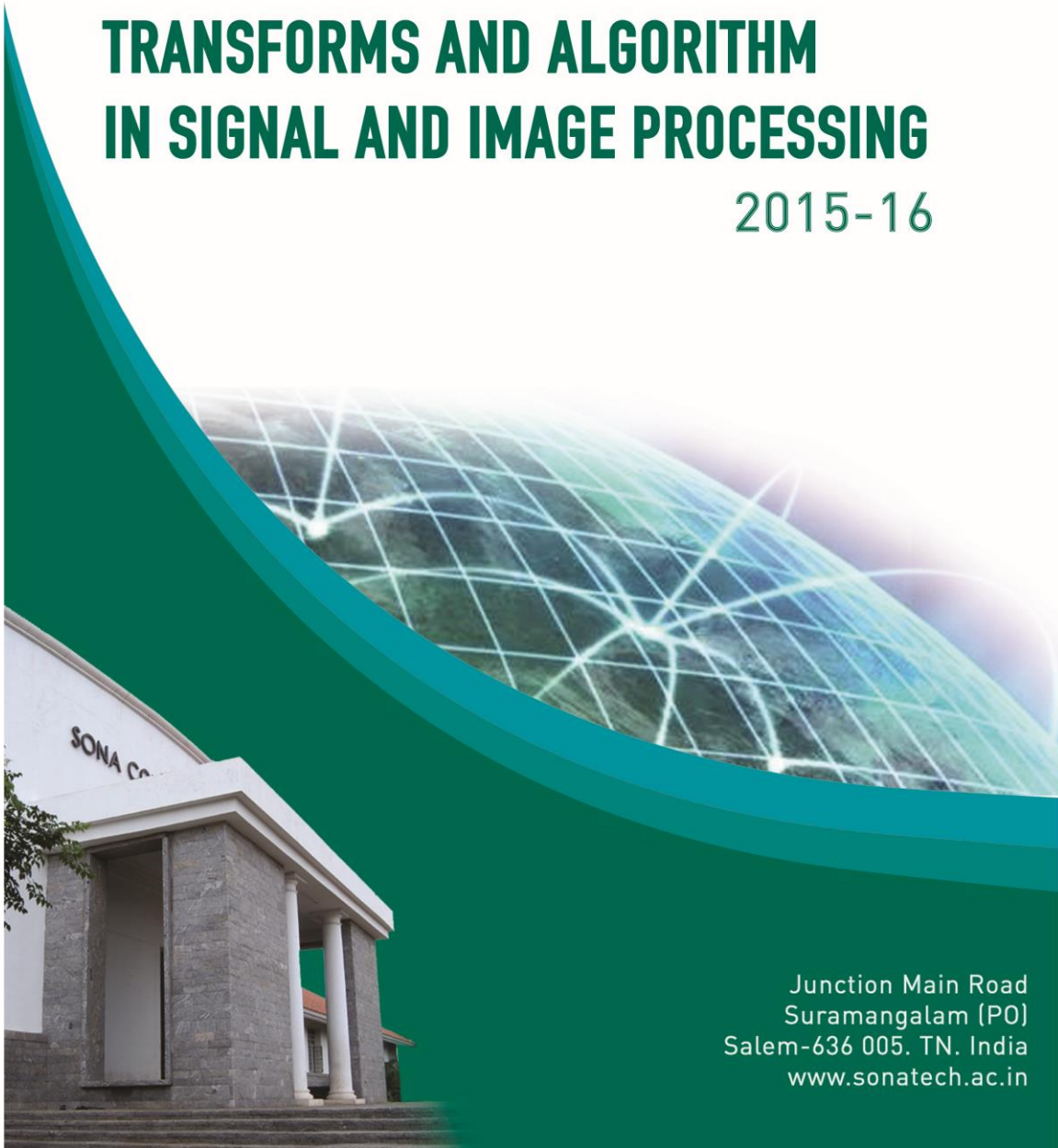
| An Autonomous Institution |

**Department of Electronics and
Communication Engineering**



TRANSFORMS AND ALGORITHM IN SIGNAL AND IMAGE PROCESSING

2015-16



Junction Main Road
Suramangalam (PO)
Salem-636 005. TN. India
www.sonatech.ac.in

EDITOR'S BOARD

Editorial Head

Dr.K.R.Kashwan,
Professor and Head, Dept
of ECE.



Editorial members:

1. Dr.R.S.Sabeenian,
Professor & Head
R&D Sona SIPRO.



2. Ms.M.Jamuna Rani,
Assist.Professor(Sr.G)



3. Dr.K.R.Kavitha,
Associate Professor



4. Ms.T.Shanthi,
Assist.Professor(Sr.G)



Magazine

Coordinator

M.Senthil Vadivu,
Assistant Professor/ECE



Student Members:

1. Akshaya.R



2. Anandhy.M



Preface

The field of signal and image processing encompasses the theory and practice of algorithms and hardware that convert signals produced by artificial or natural means into a form useful for a specific purpose. The signals might be speech, audio, images, video, sensor data, telemetry, electrocardiograms, or seismic data, among others; possible purposes include transmission, display, storage, interpretation, classification, segmentation, or diagnosis.

Current research in digital signal processing includes robust and low complexity filter design, signal reconstruction, filter bank theory, and wavelets. In statistical signal processing, the areas of research include adaptive filtering, learning algorithms for neural networks, spectrum estimation and modeling, and sensor array processing with applications in sonar and radar. Image processing work is in restoration, compression, quality evaluation, computer vision, and medical imaging. Speech processing research includes modeling, compression, and recognition. Video compression, analysis, and processing projects include error concealment technique for 3D compressed video, automated and distributed crowd analytics, stereo-to-auto stereoscopic 3D video conversion, virtual and augmented reality.

TABLE OF CONTENTS

S.No	Title	Page No
1.	BILATERAL FILTER	5
2.	BLIND NOISE ESTIMATION PRINCIPLES	7
3.	DISTRIBUTED RADAR SENSING	11
4.	OPTICAL SIGNAL PROCESSING	12
5.	STREAM FLOW CHARACTERIZATION AND FEATURE DETECTION USING A DISCRETE WAVELET TRANSFORM	19
6.	WAVELET SPECTRAL ANALYSIS OF DAILY STREAM FLOW RECORDS	21
7.	AUTOMATIC DETECTION OF EPILEPTIC SEIZURES IN EEG USING DISCRETE WAVELET TRANSFORM AND APPROXIMATE ENTROPY	23

BILATERAL FILTER

Kanimozhi.R.K – IV Year

The bilateral filter is a robust edge-preserving filter introduced by Tomasi and Manduchi. It has been used in many image processing and computer vision tasks. A bilateral filter has two filter kernels: a spatial filter kernel and a range kernel for measuring the spatial and range distance between the center pixel and its neighbors, respectively. The two filter kernels are traditionally based on a Gaussian distribution. Being non-linear, the brute force implementations of the bilateral filter are slow when the kernel is large. In the literature, several techniques have been proposed for fast bilateral filtering. The bilateral filter can be implemented as a separable operation. The cost of this approach is still high for large kernels. Using local histogram and ignoring the spatial filter kernel, the computational complexity of the bilateral filter can be greatly reduced and can be independent of the filter kernel size when integral histogram is used. Linearize the bilateral filter by quantizing the range domain to a small number of discrete values. The input image in a volumetric data structure can be represented as a bilateral grid. The use of bilateral grid increases the accuracy when the spatial domain quantization is included. Its parallel implementation demonstrates real-time grayscale image filtering performance even for high-resolution images. However, the memory cost maybe unacceptable when filter kernel is small. These methods work efficiently only on grayscale images.

Gaussian KD-trees for efficient high-dimensional Gaussian filtering:

Let N denote the number of image pixels, and D denote the number of channels, its computational complexity is $O(N \log(N)D)$ and the memory complexity is $O(N D)$. This method can be directly integrated for fast bilateral filtering. Permutohedral lattice has a computational complexity of $O(N D^2)$ and is faster than their Gaussian KD-trees for relatively lower dimensionality but has a higher memory cost. However, these methods all rely on quantization and may sacrifice accuracy for speed. Inspired by the bilateral filter, a number of edge-preserving filtering methods that have similar applications, but lower computational complexity emerges recently. A recursive approximation of the bilateral filter is that instead of the spatial filter kernel, the range filter kernel is constrained. A traditional range kernel measures the range distance between the center pixel p and another pixel q based on their color difference. However, the proposed method measures the range distance between p and q by accumulating the color difference between every two neighboring pixels on the path between p and q . For any bilateral filter containing this new range filter kernel and any spatial filter kernel that can be recursively implemented, a recursive implementation can be obtained by simply altering the

coefficients of the recursive system defined by the spatial filter kernel at each pixel location. The computational and memory complexity of the proposed recursive approximation are both $O(ND)$. It is more efficient than the state-of-the-art bilateral filtering methods that have a computational complexity of $O(N D^2)$ or $O(N \log(N)D)$. Specifically, the implementation takes about 35 ms to process a one-megapixel color image (and about 12 ms to process a 1-megapixel grayscale image). The experiments were conducted on a 3.2 GHz Intel Core i7 CPU. The memory complexity of the proposed implementation is also low: as few as the image memory will be required (memory for the images before and after filtering is excluded).

BLIND NOISE ESTIMATION PRINCIPLES

M.Suriya – IV year

SFD (signal and frequency dependent) Noise Model (The Theoretical Assumptions)

1) A Signal Dependent Model:

The image formed at the CFA contains noise that depends on the intensity of the underlying image. This intensity dependence of the noise model remains until the last step of the camera processing chain (JPEG encoding). The value of the tabulated gamma correction function is generally unknown. Even when this information is available, the CCD or CMOS detectors do not necessarily follow a simple linear relation intensity/variance when acquired at the CFA. Therefore, the noise estimation algorithm must estimate intensity-dependent noise. A common alternative is to transform the data into homoscedastic noise via an Anscombe transform. Yet an Anscombe transform is only possible for raw images. In the general setting of a signal dependency that can be different for every frequency, there is Algorithm 1 SFD Noise Estimation no other way to estimate the signal dependent noise model than dividing the set of blocks into disjoint bins, each for a different intensity and to estimate a separate frequency-dependent noise model on each intensity bin.

Assumption 1:

The noise model is intensity dependent. Therefore, it can only be estimated on groups of patches having the same intensity. It is possible to adapt most patch-based homoscedastic noise estimation methods to measure intensity-dependent noise, by simply splitting the list of input blocks into sets of blocks disjoint in mean intensity (bins) as will be done in lines 4-15 of Algorithm 1.

Algorithm 1 SFD Noise Estimation

- 1: **Input** : Noisy image \mathbf{u} of size $N_x \times N_y$ pixels.
- 2: **Input** : $w \times w$ size of the block in pixels.
- 3: **Output** : SFD noise curve $\hat{\sigma}$.
- 4: Extract from the input image all possible M overlapping $w \times w$ blocks m_k and compute their 2D orthonormal DCT-II, $\tilde{m}_k, k \in \{0 \dots M - 1\}$.
- 5: Set $\mathbf{L} = \emptyset$ ▷ Empty set.
- 6: **for** each reference DCT block $\tilde{m}_R, R \in \{0 \dots M - 1\}$,
do
- 7: $\mathbf{S} = \text{sd_freqs}(\tilde{m}_R)$ ▷ Def. 2
- 8: Find block \tilde{m}_C that minimizes sparse distance $\text{SD}_{\tilde{m}_R, \tilde{m}_C}$ with frequencies \mathbf{S} ▷ Eq. 1
- 9: Extract from $\tilde{m}_R[0, 0]/w$ the mean of m_R .
- 10: $\mathbf{L} \leftarrow [\tilde{m}_R, \text{SD}_{\tilde{m}_R, \tilde{m}_C}]$ ▷ Append
- 11: **end for**
- 12: Classify the elements of list \mathbf{L} into disjoint bins according to the mean intensity of the blocks.
- 13: **for** each bin, **do**
- 14: Obtain the set \mathbf{S}_p made by those DCT blocks in \mathbf{L} in the current bin whose SD is below the p -quantile, with $p = 0.005$.
- 15: Assign intensity I to current bin. ▷ Eq. (4)
- 16: **for** each frequency $[i, j]$ with $[i, j] \in [0, w - 1]^2, [i, j] \neq [0, 0]$, **do**
- 17: Compute the (biased) STD of the noise $\hat{\sigma}[I][i, j]$ at the current bin for frequency $[i, j]$ using the MAD estimator, using the blocks in \mathbf{S}_p . ▷ Eq. (2)
- 18: Correct the biased $\hat{\sigma}[I][i, j]$ and obtain the final STD estimate. ▷ Eq. (3)
- 19: **end for**
- 20: **end for**

2) Dealing with Frequency Dependency (The DCT Diagonal Assumption):

The main assumption underlying the algorithm is that the unknown linear and nonlinear transforms that have been applied to the image can be approximated by a diagonal operator on the DCT patch coefficients. There are two arguments in favor of an (approximately) diagonal operator. The first one is based on the following proposition (its proof is straightforward).

Proposition 1: Every linear real symmetric filter applied to an image is a diagonal operator on the DCT transform.

Because of boundary effects, this result is only approximately true for the (local) block DCT. Second, JPEG 1985 also is a diagonal (nonlinear) operator on the DCT coefficients. The denoising operation itself is an edge adaptive complex operation, but on smooth noisy regions it is close to a linear isotropic interpolator, which again is a diagonal operator. This leads us to the second assumption.

Assumption 2:

A noise patch model is fully described by the variances of its DCT coefficients. These variances also depend on the patch (average) intensity (Assumption 1). 3) Definition of the SFD Noise Model: The proposed signal and frequency dependent (SFD) noise model follows from Assumptions 1 and 2.

Definition 1: For each patch size w and each color channel we call SFD model a function

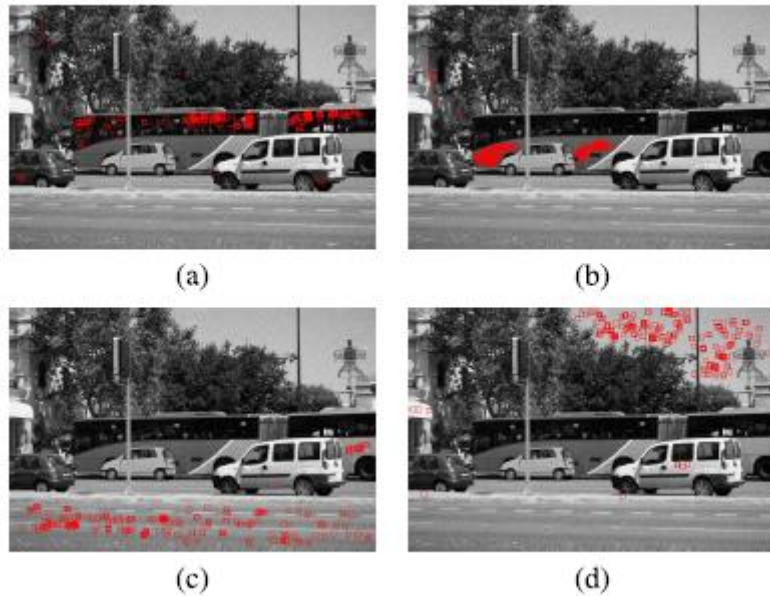
$$(i, j, b) \in [[0, w - 1]]^2 \times [0, B - 1] \rightarrow \sigma(i, j, b),$$

where (i, j) is the DCT frequency, w the block size, B the number of intensity level bins, b the current bin, and $\sigma(i, j, b)$ the observed noise standard deviation for this frequency and bin.

To estimate an SFD model, it is enough to find sufficiently many noise patches in a given image, and to apply to them a DCT before measuring the variance of their DCT coefficients.

B. Finding Patches with Only Noise Blocks

With minimal variance extracted from the image are likely to contain no signal, and therefore only noise. This is the low variance principle. The idea is to associate with each block its most similar block in a neighborhood. Then, if this similarity is essentially caused by the signal, the difference of both blocks becomes a pure noise block, with twice the variance of the original noise. In practice, however, most of the selected blocks correspond to flat zones.



This leads us in the next paragraph to refine the selection of noisy patches.

1) A Sparse Semi-Distance between Patches:

The patch distance is computed on the patches after applying to them a DCT. Such patches DCT patches and denote them by m . The distance of two DCT patches is computed on a random subset of half the DCT frequencies when estimating the other half, and conversely. But the use of a patch distance will be different. To detect noise patches by comparing them to other patches and enhancing any suspicious similarity, interpreted as the presence of signal in the patch. To find first for each DCT patch $m \sim R$ a subset of frequencies S (one fourth of the frequencies) that are the most likely to represent the patch geometry. To obtain the relevant frequencies for a given reference patch $m \sim R$, all surrounding candidate patches $m \sim C$ at a valid (taxi driver) distance r satisfying $r_1 = 4 < r < r_2 = 14$ are analyzed in order to find the frequencies whose coefficients exhibit the largest variation. The condition $r_1 < r$ is to avoid an excessive overlapping between the reference and the chosen blocks, to be able to properly estimate spatially correlated noise. The condition $r < r_2$ is to reduce the search area, since block matching is computationally expensive.

Definition 2 (Relevant Frequencies):

For each reference patch $m \sim R$ and a neighboring patch $m \sim C$ at valid distance, we say that (i, j) is a relevant frequency for comparison of $m \sim R$ and $m \sim C$ if $|\tilde{m}_R[i, j] - \tilde{m}_C[i, j]|$ is among the $w_2/4$ first such values in decreasing order. Set $H(i, j)$ as the number of times (i, j) has been retained as valid for all neighboring patches $m \sim C$. We say that (i, j) is a relevant frequency

for \tilde{m}_R if it is associated with one of the $w^2/4$ highest values of $H(i, j)$. The set of relevant frequencies of \tilde{m}_R will be denoted by S . Definition 3: The sparse distance¹ between \tilde{m}_C and \tilde{m}_R is defined by

$$SD_{\tilde{m}_R, \tilde{m}_C} = \sum_{(i,j) \in S(\tilde{m}_R)} |\tilde{m}_R[i, j] - \tilde{m}_C[i, j]| \times \max(|\tilde{m}_R[i, j]|, |\tilde{m}_C[i, j]|).$$

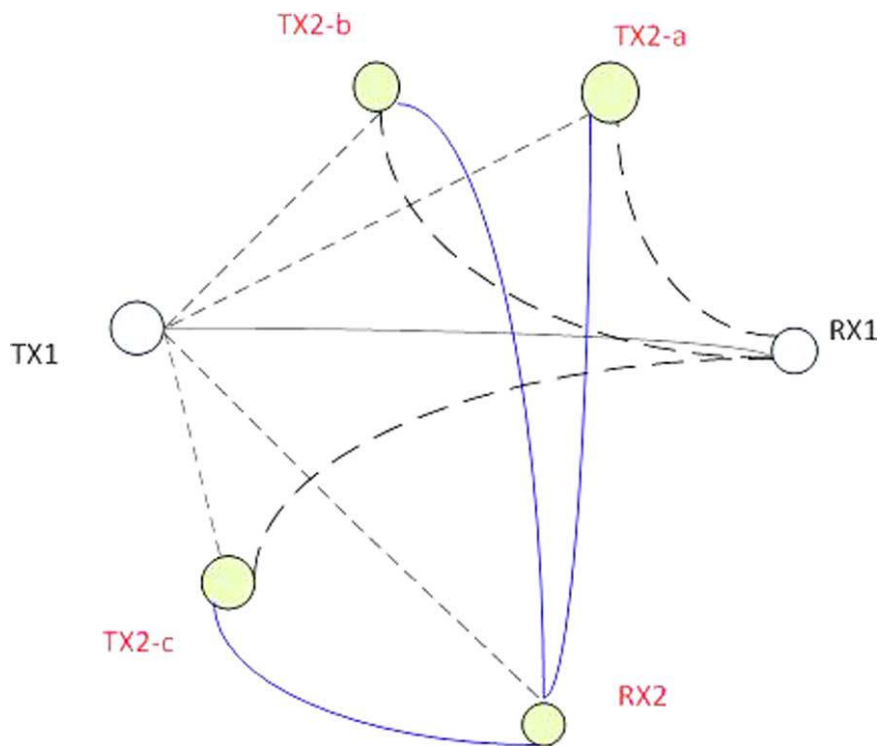
Given the set of relevant frequencies S for \tilde{m}_R , the first factor of the distance, $|\tilde{m}_R[i, j] - \tilde{m}_C[i, j]|$, penalizes the absolute difference of the DCT coefficients in the blocks (the DCT coefficients of similar blocks should be similar). The second factor, $\max(|\tilde{m}_R[i, j]|, |\tilde{m}_C[i, j]|)$ adds more penalty when the absolute value of the coefficient is higher. Indeed, the definition of S suggests that the higher the absolute value of the coefficient, the more contribution it has to the geometry of the patch. The sparse distance is designed so as to enhance any non-casual resemblance with neighboring blocks, being computed on the set of relevant frequencies of \tilde{m}_C only. Our principle is that the blocks showing the smallest sparse distance to their neighbors are more likely than others to be pure noise blocks. Fig. 2 shows the blocks selected by Algo. 1 using the sparse distance

DISTRIBUTED RADAR SENSING

Akshaya.R – IV Year

Distributed Radar Sensing is a rapidly growing research area and has recently received much attention from the research community. This is mainly because of information limit of monostatic radars and their single angle perspective of the target. Distributed radar system provides potential advantages such as improving coverage of large areas (e.g., solving blockage effects), improving detection performance, and higher 2D (angular) resolution-as distributed radar can probe targets from different aspects and can exploit the spatial diversity of radar targets for a better detection performance- solving inherent radar problems (such as blind speed or Doppler shift problem, aspect angle), possibility of imaging and target feature extraction, greater immunity to jamming, as well as the low-power low-complexity radar sensors instead of a high power complex radar. Other advantages are resilience to fading, and graceful degradation. The disadvantages of distributed radar network are the interference among radar emitters, the requirement of precise location information of sensing nodes, the synchronization problem of radar sensors and the need for data fusion of many simple types of radar. In this paper we concentrate on the interference issue of distributed radar networks. Distributed radar sensing network relies on waveforms or signals to unleash its performance potential. To this end, the signal design issue is focused in this paper and particularly based on wavelet packet modulation technique as wavelets provide flexibility in signal design in distributed radar networks. In addition to flexibility, the reconfigurability of wavelet signals is also important which paves the way for their successful application in cognitive radar networks. Wavelets have been favorably applied in various aspects of radar systems including target detection, parameters estimation, feature extraction, classification, Synthetic Aperture Radar (SAR) image compression, clutter removal, target extraction from clutter, radar signal denoising, data compression, side lobe reduction and interference suppression. The usage of wavelet-based waveforms for search and tracking operations of radar is proposed, where the waveforms adjust the bandwidth and transmit power adapting to the target and environmental conditions. The main property of wavelets in these applications is in their flexibility and ability to characterize signals accurately. Wavelet transform, as a possible analysis technique when designing radar systems, provides advantages such as flexibility, lower sensitivity to distortion and interference, and better utilization of spectrum. In a distributed radar system several radars operate in a network and share the spectrum (see Fig. 1). The fundamental geometry of the radar network can be bistatic or monostatic. A radar node in the distributed radar network can be a transmitter, a receiver, or both a transmitter and a receiver. The idea is the use of different waveforms by radars concurrently sharing the spectrum such that a particular receiver can separate the resulting received signal and perform target detection. As radars share the

spectrum in order to avoid interference among radars their signals should be orthogonal. This orthogonality is the key characteristic of the distributed radar network. Furthermore, for a high resolution in multiple target detection, the transmitted signals should have low correlation side lobes levels. The orthogonality can be provided by transmission on orthogonal subcarriers. The Pandora signal consists of several linear narrowband \FM (LFM) separated by guard bands. The output signal of LFM bands are combined in the radar receiver and providing a high resolution. A proper replacement of LFM is the Orthogonal Frequency Division Multiplexing (OFDM) where it has been proven that OFDM-coded radar waveforms are comparable with LFM waveforms and furthermore, experience no range-Doppler coupling. The main advantages of OFDM are its robustness against multipath fading, relatively simple synchronization processing and its spectral efficiency. By coding of OFDM radar signal side lobes of the ambiguity function are also reduced. A joint radar and wireless communication system for future intelligent transportation networks is proposed where an OFDM signal is designed for joint communication and radar functionality and the possibility of estimating the relative velocity and efficient implementation based on fast Fourier transforms is shown.



An alternative approach to the OFDM scheme is to exploit the orthogonal properties of wavelet packet based basis functions. In this technique the Fourier based orthogonal signals of OFDM are replaced with wavelet packets. The main advantages of using wavelets are their ability and flexibility to characterize radar signals with adaptive time-frequency resolution. In fact unlike OFDM modulation which divides the whole bandwidth into orthogonal and

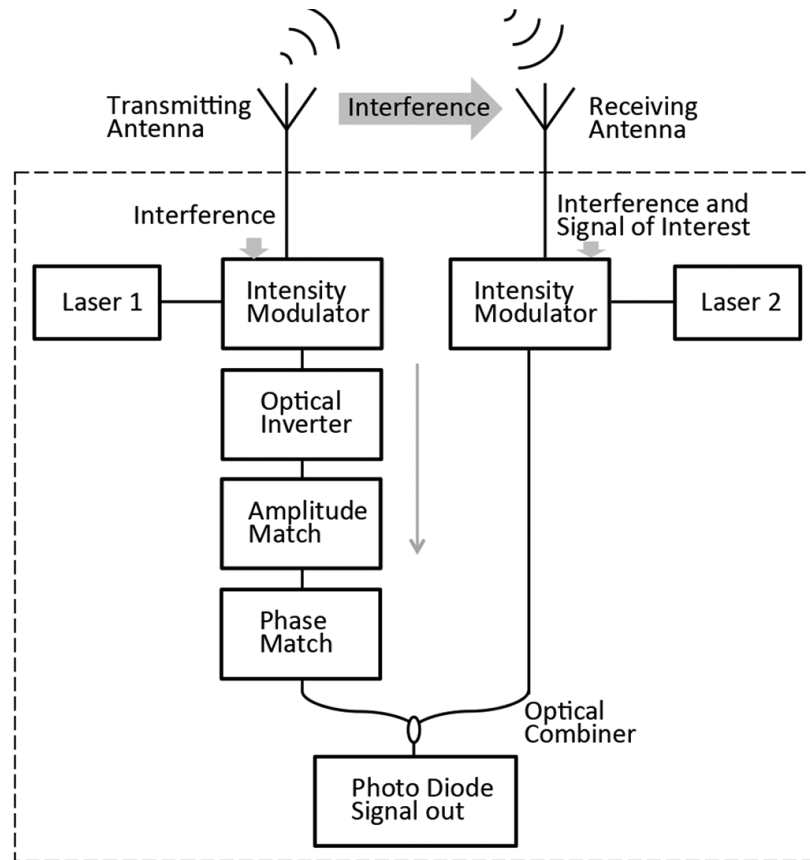
overlapping sub bands of equal bandwidths, Wavelet packets modulation (WPM) assigns wavelet sub bands having different time and frequency resolutions. Furthermore, WPM is more robust to interference (an extremely important issue when it comes to distributed radar networks where the radar nodes interfere each other) as well as multipath propagation. Wavelet packet signals are more spectrally efficient than OFDM and moreover the advantage of wavelet transform lies in its flexibility to customize and shape the characteristics of the waveforms for joint radar and communication functionalities.

OPTICAL SIGNAL PROCESSING

M. Nivetha – III Year

A. Analog Noise Protected Optical Encryption

Interference is undesirable when transmitting and receiving data. However, if the interference can be controlled, its noise like signature can be used to effectively carry out encryption. Interference cancellation techniques are especially important for wireless communication. If a wireless router transmits and receives signals at the same time, the transmitting antenna generates unwanted interference for the receiving antenna. Because the transmitting antenna is much closer than the source of the signal of interest, the amplitude of interference is usually much larger than the amplitude of the signal. A technique to cancel the interference in which the transmitting antenna is connected internally through a fiber link with the receiving antenna. The fiber link includes two channels with two lasers and converts the electric signals from both the transmitting antenna and receiving antenna into optical signals by intensity modulation. The signal from the receiving antenna contains both the signal of interest and the interference, while the signal from the transmitting antenna only contains interference. The fiber link can invert the signal from the transmitting antenna using optical devices and sum the signals from the two antennas. Since the signal from the transmitting antenna is inverted, it can cancel the interference from the receiving antenna. The benefit of using the fiber link for interference cancellation is not only that it achieves high speed and real-time processing, but also that it reaches a high cancellation ratio of 30 dB. The challenge for this method is that the phases and amplitudes of the interference in the two channels must be precisely matched in order to be canceled by each other. If either phase or amplitude is not matched, the cancellation ratio will decrease significantly with the mismatch. Both the benefit and challenge of this cancellation technique are benefits if this technique is applied as an encryption method. The interference noise can serve as analog noise accompanying the transmitted signal. The precise requirement of amplitude and phase matching can be used as the key for the encryption process. The high-speed property of the fiber optic processing method satisfies the requirement of large bandwidth and real time processing of the signal encryption. In our experiment, we have achieved 10 Gb/s encrypted data transmission with real time encryption in a 25 km fiber link



Schematic diagram of interference cancellation.

The signal is disguised as natural analog noise, and only by matching both the amplitude and phase of the analog noise between transmitter and receiver can the receiver decrypt the signal. The analog noise shares the same frequency range with the signal, so that the noise cannot be removed by filters. If the eavesdropper cannot find the matching condition, the signal cannot be digitized. If the signal cannot be decrypted when being received, the data is lost and cannot be recovered by a post-processing technique. The schematic diagram of the encryption system reveals that the transmitter is very similar to the interference cancellation system (Fig. 2). The only difference is that, in the interference cancellation system, the amplitude and phase are designed to be matched, while in the transmitter of the encryption system, the amplitude and phase differences are generated deliberately, so both of the parameters can be used as keys for encryption. The signals in Channel 1 and Channel 2 can be described as:

$$C_1 = S_1 + N_1.$$

$$C_2 = N_2.$$

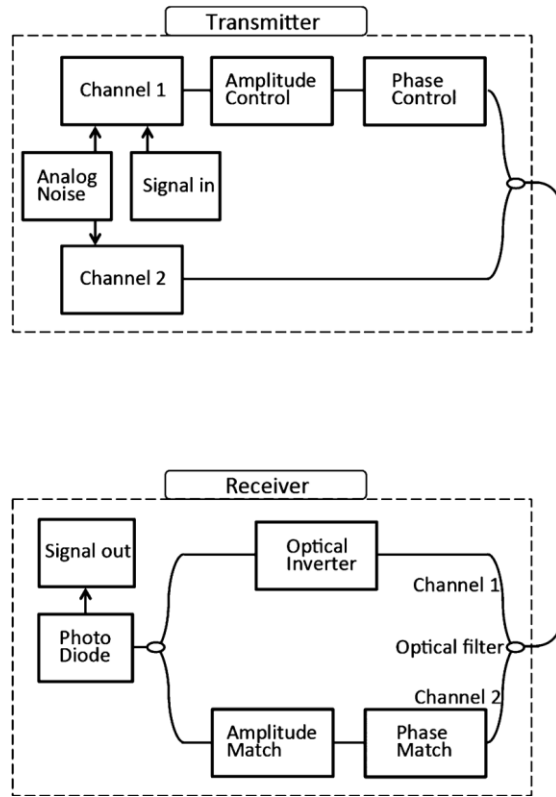


Fig. 2. Schematic diagram of analog noise encryption system.

where S_1 is the transmitted signal and N_1 is the interference noise in channel 1. N_2 is the cancellation noise in channel 2. To decrypt the signal, the amplitude and phase of and have to be matched at the receiver. When the interference is cancelled by the receiver, a clear eye diagram is received; when the interference is not cancelled, the signal is noisy and cannot be digitized. This technique is also suitable for multi-user wavelength division multiplexing (WDM) systems. For a single user, the encryption system needs two channels with different wavelengths. In the case of a multi-user WDM system, the different users deploying multiple WDM channels can share the same channel for carrying the analog noise used for cancellation. Different WDM channels can use different keys for the encryption, which means different amplitude and phase of the interference noise signal is applied.

STREAM FLOW CHARACTERIZATION AND FEATURE DETECTION USING A DISCRETE WAVELET TRANSFORM

Sarathy Ramadoss – IV Year

An exploration of the wavelet transforms as applied to daily river discharge records demonstrates its strong potential for quantifying stream flow variability. Both periodic and non-periodic features are detected equally, and their locations in time preserved. Wavelet Scalograms often reveal structures that are obscure in raw discharge data. Integration of transform magnitude vectors over time yields wavelet spectra that reject the characteristic time-scales of a river's flow, which in turn are controlled by the hydroclimatic regime. For example, snowmelt rivers in Colorado possess maximum wavelet spectral energy at time-scales on the order of 4 months owing to sustained high summer flows; Hawaiian streams display high energies at time-scales of a few days, reacting the domination of brief rainstorm events. Wavelet spectral analyses of daily discharge records for 91 rivers in the US and on tropical islands indicate that this is a simple and robust way to characterize stream flow variability. Wavelet spectral shape is controlled by the distribution of event time-scales, which in turn reacts the timing, variability and often the mechanism of water delivery to the river. Five hydroclimatic regions, listed here in order of decreasing seasonality and increasing pulsatory nature, are described from the wavelet spectral analysis: (a) western snowmelt, (b) north-eastern snowmelt, (c) mid-central humid, (d) southwestern arid and (e) 'rainstorm island'. Spectral shape is qualitatively diagnostic for three of these regions. While more work is needed to establish the use of wavelets for hydrograph analysis, our results suggest that river flows may be effectively classified into distinct hydroclimatic categories using this approach.

Spring snowmelt in a north-eastern US river Rivers in the north-eastern US tend to experience a significant increase in flow each spring from the melting of accumulated winter snow. However, this structure is commonly obscured by rainstorm events throughout the year, as illustrated by a seven-year subset of the daily discharge record for the Ammoniac River, Maine (Figure 2c). Transform magnitude vectors for wavelets of scale a (1; 2; 4; 8; 16; 32; 64; 128) days, corresponding to feature scales of approximately {2, 4, 8, 16, 32, 64, 128 and 256} days are shown in Figure 2a. These vectors are contoured with a single threshold of $5 \times 10^{-6} \text{ m}^3/\text{s}$ in Figure 2b: intensities above this level appear in black, lower values are not contoured. The wavelet Scalogram of this subset seven-year discharge record reveals seven spring snowmelt events (which are of longer duration than rainstorms) as large blobs centered around feature scales of 64 ± 128 days (Figure 2b). Note that time is preserved on the x-axis, feature scale (event duration) increases along the y-axis and transform intensity rises out of the page. Numerous studies have utilized the scale and timing of snowmelt features to identify the

hydrological regimes of northern watersheds (see Woo, 1990). Wavelet transformation of daily discharge time-series permits clear identification of diagnostic structures that may be obscure in the raw data, while wavelet spectral analysis (described in the section on analysis of stream flow records) provides easy assimilation and comparison of long records for numerous rivers.

WAVELET SPECTRAL ANALYSIS OF DAILY STREAM FLOW RECORDS

M.Surya – III Year

Integrating each transform magnitude vector over time to obtain the total energy at each wavelet scale permits construction of spectral curves that reflect the distribution of event time-scales contained in the signal. Wavelet spectra are like Fourier spectra in that the temporal location of specific features is lost; the distribution of event scales is instead summarized for the entire input signal. Wavelet Scalograms, which preserve the temporal locations of events, should be used to describe flow variability in non-stationary discharge hydrographs. For rivers that do not display long-term changes in stream flow structure, wavelet spectra are useful for summarizing a river's temporal variability and comparing it with flows in other rivers.

The wavelet transform is a powerful tool for hydrograph analysis, both for identifying transient features and quantifying the temporal variability of stream flow. Wavelet Scalograms permit precise location of both stochastic and periodic events in time and may reveal subtle structures not easily seen in the raw discharge data. Integration of Scalograms over time permits construction of wavelet spectral curves that reflect the distribution of event time-scales and are diagnostic of hydroclimatic regime. Wavelet spectral curves for 91 rivers from five different climatic regions in the US and on tropical islands are strongly similar within the same region but differ between regions. More work is needed to establish wavelet transformation as a viable and consistent tool for hydrological time-series analysis. Remaining issues include determining which wavelet scales are most sensitive to climatic signatures, how to quantify the relationship between spectral shape and hydroclimatic regime and how the choice of wavelet and sampling rate affects results. However, our first exploration of the topic suggests that river flows may be effectively classified by hydroclimatic regime from the shape of their spectra, or by combining spectral curves with structural information from wavelet Scalograms.

AUTOMATIC DETECTION OF EPILEPTIC SEIZURES IN EEG USING DISCRETE WAVELET TRANSFORM AND APPROXIMATE ENTROPY

D.Kabilan – IV Year

In this study, a new scheme was presented for detecting epileptic seizures from electroencephalogram (EEG) data recorded from normal subjects and epileptic patients. The new scheme was based on approximate entropy (ApEn) and discrete wavelet transform (DWT) analysis of EEG signals. Seizure detection was accomplished in two stages. In the first stage, EEG signals were decomposed into approximation and detail coefficients using DWT. In the second stage, ApEn values of the approximation and detail coefficients were computed. Significant differences were found between the ApEn values of the epileptic and the normal EEG allowing us to detect seizures with over 96% accuracy. Without DWT as preprocessing step, it was shown that the detection rate was reduced to 73%. The analysis results depicted that during seizure activity EEG had lower ApEn values compared to normal EEG. This suggested that epileptic EEG was more predictable or less complex than the normal EEG. The data was further analyzed with surrogate data analysis methods to test for evidence of nonlinearities. It was shown that epileptic EEG had significant nonlinearity whereas normal EEG behaved like Gaussian linear stochastic process.

Wavelet transforms are widely applied in many engineering fields for solving various real-life problems. The Fourier transform of a signal contains the frequency content of the signal over the analysis window and, as such, lacks any time domain localization information. To achieve time localization information, it is necessary for the time window to be short, therefore compromising frequency localization. On the contrary to achieve frequency localization requires large time analysis window and time localization is compromised. Therein lies the dilemma, sometimes referred to as the “uncertainty principle”. The short-time Fourier transform (STFT) represents a sort of compromise between the time and frequency-based views of a signal and contains both time and frequency information. STFT has a limited frequency resolution determined by the size of the analysis window. This frequency resolution is fixed for the entire frequency band. The EEG data used in this study consists of four different sets. The first set includes surface EEG recordings that were collected from five healthy subjects using a standardized electrode placement scheme. The subjects were awake and relaxed with their eyes open. The data for the last three sets was obtained from five epileptic patients undergoing presurgical evaluations. The second and the third data sets consist of intracranial EEG recordings during seizure free intervals (interictal periods) from within the epileptogenic zone and opposite the epileptogenic zone of the brain, respectively. The data in the last set was recorded during seizure activity (ictal periods) using depth electrodes placed within the epileptogenic zone.